Hydrogel Scaffolds with Immobilized Bacteria for 3D Cultures

María C. Gutiérrez,[†] Zaira Y. García-Carvajal,[†] Matías Jobbágy,[†] Luis Yuste,[‡] Fernando Rojo,[‡] Concepción Abrusci,[§] Fernando Catalina,[⊥] Francisco del Monte,*[,†] and María L. Ferrer[†]

Institute of Materials Science at Madrid (ICMM) and Biotechnology National Center (CNB), Spanish Research Council (CSIC), Cantoblanco, 28049 Madrid, Spain, Institute of Polymers Science and Technology (ICTP), Spanish Research Council (CSIC), Juan de la Cierva, 7. 28006 Madrid, Spain, and Department of Microbiology III, Faculty of Biology, University Complutense of Madrid, José Antonio Novais, 2. 28040 Madrid, Spain

Received December 5, 2006. Revised Manuscript Received January 25, 2007

We have studied the suitability of a cryogenic process (e.g., ice-segregation-induced self-assembly, ISISA) for preparation of polyvinyl alcohol (PVA) scaffolds with in situ immobilized bacteria (e.g., *Escherichia coli*). Confocal fluorescence microscopy and impedance measurements were used to evaluate the extension of bacteria proliferation within the scaffold macrostructure. The bacteria efficiency for colonization of the scaffold macrostructure is compared for bacteria immobilized with and without the use of additional cryoprotectans. Cryoprotection by bacteria entrapment in alginate beads containing glucose results in a significant improvement (more than 2-fold as compared to non-cryoprotected) of bacteria proliferation within the PVA scaffold. Results are also compared with the most widely used method for cells colonization of scaffolds; i.e., soaking of a preformed PVA scaffold in bacteria culture medium.

Introduction

The pressures of an ever-increasing population and industrial development have led to the addition of an array of man-made chemicals in the environment, leading to tremendous deterioration in environmental quality. Contamination of soil, air, water, and food is one of the major problems facing the industrialized world today. Significant regulatory steps have been taken to eliminate or reduce production and/or release of these chemicals into the environment. Microbial cells and bacteria are being widely used for bioremediation and biocatalysis, offering the possibility to decontaminate polluted environmental media and implement chemo-enzymatically catalyzed, environmentally friendly synthetic methods.[1]

Immobilization of microbial cells in membranes and bioreactors provides enhanced catalytic activity and stability, protecting microorganisms from mechanical degradation and deactivation and allowing for an overall intensification of biochemical reactions.[2] Such membranes and bioreactors must indeed be suitable supports for cells growth, which implies they must be composed of biocompatible materials and processed into a porous matrix of suitable morphology (e.g., scaffolds).[3] Cell immobilization typically occurs after scaffold preparation (e.g., by soaking the scaffold into a cell suspension), which eventually makes cells proliferate within the whole scaffold structure difficult. Note that the presence of the support itself introduces mass transfer restrictions for the diffusion of any substance (nutrients and oxygen, among others), which impedes cell proliferation deep inside the scaffold.[4] This event (e.g., cell proliferation within the scaffold limited to just a few layers of cells) has also been corroborated for animal cells growing in inverted colloidal crystals, for which rational design is ideal for the study of cell−cell and cell−matrix interactions, cell growth, and cell motility.[5] This problem can be overcome if cells grow from the inner to the outer side of the scaffold, in search of nutrients and oxygen. For this purpose, one should design chemical processes suitable for preparation of scaffolds with in situ immobilized cells. Unfortunately, the vast majority of preparation processes devised so far to prepare scaffolds (phase emulsion, air bubbling, or use of templates, among

* Corresponding author. E-mail: delmonte@icmm.csic.es. Phone: 34 91 3349033. Fax: 34 91 3720623.
[†] Institute of Materials Science at Madrid, Spanish Research Council.
[‡] Biotechnology National Center, Spanish Research Council.
[§] University Complutense of Madrid.
[⊥] Institute of Polymers Science and Technology, Spanish Research Council.

(1) (a) Ishige, T.; Honda, K.; Shimizu, S. *Curr. Opin. Chem. Biol.* **2005**, *9*, 174. (b) White, C.; Sharman, A. K.; Gadd, G. M. *Nat. Biotechnol.* **1998**, *16*, 572. (c) Schmid, A.; Dordick, J. S.; Hauer, B.; Kiener, A.; Wubbolts, M.; Witholt, B. *Nature* **2001**, *409*, 258.
(2) (a) Hecht, V.; Langer, O.; Deckwer, W. D. *Biotechnol. Bioeng.* **2000**, *70*, 391. (b) Pekdemir, T.; Keskinler, B.; Yildiz, E.; Akay, G. *J. Chem. Technol. Biotechnol.* **2003**, *78*, 773. (c) Giorno, L.; Drioli, E. *TIBTECH* **2000**, *18*, 339. (d) Erhan, E.; Keskinler, B.; Akay, G.; Algur, O. F. *J. Membr. Sci.* **2002**, *206*, 361. (e) Kwak, M. Y.; Rhee, J. S. *Biotechnol. Bioeng.* **1992**, *39*, 903.
(3) (a) Yang, J.; Webb, A. R.; Ameer, G. A. *Adv. Mater.* **2004**, *16*, 511. (b) Shea, L. D.; Smiley, E.; Bonadio, J.; Mooney, D. J. *Nat. Biotechnol.* **1999**, *17*, 551. (c) Stachowiak, A. N.; Bershteyn, A.; Tzatzalos, E.; Irvine, D. J. *Adv. Mater.* **2005**, *17*, 399. (d) Zhang, Y.; Wang, S.; Eghtedari, M.; Motamedi, M.; Kotov, N. A. *Adv. Funct. Mater.* **2005**, *15*, 725. (e) Dankars, P. Y. W.; Harmsen, M. C.; Brouwer, L. A.; Van Luyn, M. J. A.; Meijer, E. W. *Nat. Mater.* **2005**, *4*, 568−574.
(4) (a) Wolffberg, A.; Sheintuch, M. *Chem. Eng. Sci.* **1993**, *48*, 3937. (b) Akay, G.; Erhan, E.; Keskinler, B. *Biotechnol. Bioeng.* **2005**, *90*, 180.
(5) (a) Kotov, N. A.; Liu, Y.; Wang, S.; Cumming, C.; Eghtedari, M.; Vargas, G.; Motamedi, M.; Nichols, J.; Cortiella, J. *Langmuir* **2004**, *20*, 7887. (b) Shanbhag, S.; Wang, S.; Kotov, N. A. *Small* **2005**, *1*, 1208.

10.1021/cm062882s CCC: $37.00
Published on Web 03/17/2007

others)[6,] are not suitable for in situ cell immobilization due to the use of solvents and/or thermal treatments that cause irreversible damage to cell integrity. Hydrogels prepared from organogelators (e.g., peptide-based hydrogels)[7] have just succeeded in this attempt.

An interesting alternative can be the use of cryogenic processes, suitable for scaffold preparation and compatible with microbial cell maintenance and viability. Herein, we describe the use of a cryogenic process recently reported by Mukai et al. to prepare microhoneycomb silica porous structures from an aqueous silica gel.[8] This cryogenic process (defined by our group as ISISA, ice-segregation-induced self-assembly) is quite versatile and allows for tailoring both the composition and the morphology of the resulting scaffold.[9] Moreover, the ISISA process is also highly biocompatible, as demonstrated by the recent immobilization of proteins and liposomes within the matter that forms the microchannelled structure.[10] In this work, the biological entity to immobilize will be *Escherichia coli* (*E. coli*) and the microchannelled structure will be polyvinyl alcohol (PVA). Colonization of the PVA scaffold by bacteria will be studied by two different means (e.g., fluorescent confocal microscopy and indirect impedance measurements), given the difficulty in studying the proliferation of immobilized bacteria by classical techniques used in solution (e.g., optical density of bacteria in suspension or plate counting, among others). For bacteria visualization at the fluorescent confocal microscope, the bacterial strain of *E. coli* used in this work is genetically engineered to express a fluorescent protein (green fluorescent protein, GFP) in response to an inducer.[11] Bacteria immobilization will be achieved by ISISA processing of a PVA solution also containing bacteria either in suspension or previously entrapped in alginate beads for further cryoprotection.[12]

Experimental Section

Materials. Polyvinyl alcohol (PVA, avg mol wt = 72 000) was purchased from Fluka. Alginic acid sodium salt (viscosity ≈ 250 cP), sodium citrate, and calcium chloride were purchased from Sigma-Aldrich. All chemical compounds were used as received. Water was distilled and deionized. For any of the cases studied in this work, bacteria were genetically engineered to express GFP, a protein that emits fluorescence centered at 510 nm (e.g., green light) for light excitation at 485 nm. Fluorescence occurs as far as bacteria remain alive. Bacteria ($\sim 1 \times 10^8$/mL) were suspended in fresh M9 minimal salts medium (58 mM $Na_2HPO_4 \cdot 12H_2O$, 22 mM KH_2PO_4, 8 mM NaCl, 18 mM NH_4Cl, 2 mM $MgSO_4$, 0.1 mM $CaCl_2$, 6 pM Vitamine B1).

Preparation of Bacteria-Glucose-Alginate Beads (BB). Sodium alginate was dissolved in a diluted minimum medium (1/10) for a sodium alginate content of 2 wt %. Glucose (20 wt %) was also added to the alginate solution for further cryoprotection (see the Supporting Information). The glucose-alginate beads loaded with bacteria (BB) were prepared by addition of 1 mL of M9 minimal salt medium containing *E. coli* (500 μL of the above cell suspension to 500 μL of diluted minimum medium) to 9 mL of the glucose-alginate solution. After stirring for 10 min, the mixture was dropped into a gently stirred solution of $CaCl_2$ at a volumetric ratio of 1/5 using a syringe equipped with a needle of 0.45 mm. The $CaCl_2$ concentrations used (e.g., 50 mM) were thus selected for bead density matching with PVA solution. Otherwise, a homogeneous distribution of beads within the scaffold monolith would not be obtained. After stirring for 10 min, the resulting BBs (of ~1 mm diameter) were washed with 50 mL of distilled and deionized water before use. The temperature was maintained at 4 °C during the whole process to avoid bacteria growth.

Preparation of PVA-Bacteria (PVA-B) and PVA-BB Buffered Suspensions. Homogeneous PVA solutions (8 wt %) were prepared by the addition of 8 g of PVA to 100 mL of hot 20 mM Tris buffer (at about 80 °C). After stirring for 3 h, the resulting solution was cooled down to 4 °C. Bacteria (0.2 mL of a 1/20 diluted suspension of bacteria in M9 minimal salts medium) or BB (20) were added to 1 mL of the PVA solution, to have a fixed bacteria amount in suspension of $\sim 1 \times 10^6$/mL.

ISISA Processing of PVA, PVA-B, and PVA-BB Buffered Suspensions for Preparation of Scaffolds (PVA-S, PVA-SB, and PVA-SBB). Every suspension (1 mL) was collected in insulin syringes and dipped at a constant rate of 5.9 mm/min into a cold bath maintained at a constant temperature of −196 °C. The unidirectionally frozen samples were freeze-dried using a ThermoSavant Micromodulyo freeze-drier. The resulting monoliths kept both the shape and the size of the insulin syringes (in this particular case) and, eventually, any container where the suspensions are collected prior freezing (see Figure S1 in the Supporting Information).

3D Cultures. PVA-S samples were soaked into a suspension of bacteria in culture medium ($\sim 1 \times 10^6$ bacteria/mL), whereas PVA-SB and PVA-SBB samples were simply soaked into the culture medium (bacteria are already immobilized within the scaffold structure). The culture medium was composed of 25 mL of M9 minimal salt medium supplemented with 50 mM sodium citrate

(6) (a) Barbetta, A.; Dentini, M.; de Vecchis, M. S.; Fillippini, P.; Formisano, G.; Caiazza, S. *Adv. Funct. Mater.* **2005**, *15*, 118. (b) Partap, S.; Rehman, I.; Jones, J. R.; Darr, J. A. *Adv. Mater.* **2006**, *18*, 501. (c) Carn, F.; Colin, A.; Achard, M.-F.; Deleuze, H.; Saadi, Z.; Backov, R. *Adv. Mater.* **2004**, *16*, 140. (d) Stachowiak, A. N.; Bershteyn, A.; Tzatzalos, E.; Irvine, D. J. *Adv. Mater.* **2005**, *17*, 399. (e) Wan, A. C. A.; Tai, B. C. U.; Leck, K.-J.; Ying, J. Y. *Adv. Mater.* **2006**, *18*, 641. (f) Mann, S. *Angew. Chem., Int. Ed.* **2000**, *39*, 3392−406. (g) Sanchez, C.; Arribart, H.; Giraud-Guille, M. M. *Nat. Mater.* **2005**, *4*, 277. (h) Sanchez, C.; Arribart, H.; Giraud-Guille, M. M. *Nat. Mater.* **2005**, *4*, 277.

(7) (a) Silva, G. A.; Czeisler, C.; Niece, K. L.; Beniash, E.; Harrington, D. A.; Kessler, J. A.; Stupp, S. I. *Science* **2004**, *303*, 1352. (b) Rajangam, K.; Behanna, H. A.; Hui, M. J.; Han, X.; Hulvat, J. F.; Lomasney, J. W.; Stupp, S. I. *Nano Lett.* **2006**, *6*, 2086. (c) Jayawarna, V.; Ali, M.; Jowitt, T. A.; Miller, A. F.; Saiani, A.; Gough, J. E.; Ulijn, R. V. *Adv. Mater.* **2006**, *18*, 611.

(8) (a) Mukai, S. R.; Nishihara, H.; Tamon, H. *Chem. Commun.* **2004**, 874. (b) Nishihara, H.; Mukai, S. R.; Yamashita, D.; Tamon, H. *Chem. Mater.* **2005**, *17*, 683.

(9) (a) Zhang, H.; Hussain, I.; Brust, M.; Butler, M. F.; Rannard, S. P.; Cooper, A. I. *Nat. Mater.* **2005**, *4*, 787. (b) Mukai, S. R.; Nishihara, H.; Shichi, S.; Tamon, H. *Chem. Mater.* **2004**, *16*, 4987. (c) McCann, J. T.; Marquez, M.; Xia, Y. *J. Am. Chem. Soc.* **2006**, *128*, 1436. (d) Deville, S.; Saiz, E.; Nalla, R. K.; Tomsia, A. P. *Science* **2006**, *311*, 515. (e) Nishihara, H.; Mukai, S. R.; Tamon, H. *Carbon* **2004**, *42*, 889.

(10) (a) Ferrer, M. L.; Esquembre, R.; Ortega, I.; Mateo, C. R.; del Monte, F. *Chem. Mater.* **2006**, *18*, 554. (b) Gutierrez, M. C.; Jobbagy, M.; Rapun, N.; Ferrer, M. L.; del Monte, F. *Adv. Mater.* **2006**, *18*, 1137.

(11) (a) Ferrer, M. L.; Yuste, L.; Rojo, F.; del Monte, F. *Chem. Mater.* **2003**, *15*, 3614. (b) Ferrer, M. L.; García-Carvajal, Z. Y.; Yuste, L.; Rojo, F.; del Monte, F. *Chem. Mater.* **2006**, *18*, 1458.

(12) (a) Korgel, B. A.; Rotem, A.; Monbouquette, H. G. *Biotechnol. Prog.* **1992**, *8*, 111. (b) Cachon, R.; Molin, P.; Diviès, C. *Biotechnol. Bioeng.* **1995**, *47*, 567. (c) Laca, A.; García, L. A.; Díaz, M. *J. Biotechnol.* **2000**, *80*, 203.

and 30 mM glucose (as carbon source). Sodium citrate is not a carbon source for *E. coli* but allows for BB liquation. For this purpose, scaffolds were maintained in culture medium at 4 °C for 60 min (bacteria growth is negligible at 4 °C). The amount of BB was fixed to have $\sim 1 \times 10^6$ bacteria/mL in the buffered suspension after bead dissolution. Thereafter, the flasks were incubated at 37 °C for 24 h under gentle stirring to allow for bacterial growth.

Indirect Impedance Measurements. The experiments were performed on a Micro-Trac 4100 (SY-LAB Geräte GmbH, Neupurkerdorf, Austria) on PVA-SB and PVA-SBB samples (after bead rehydration and dissolution). Fresh bacteria simply suspended in culture medium (at the above fixed bacteria amount, $\sim 1 \times 10^6$/mL) were also studied for comparison. Every sample was introduced under sterile conditions in 7 mL disposable cylindrical polyethylene containers containing 1 mL of culture medium. This polyethylene container is introduced into a cylindrical polystyrene container that has four stainless steel electrodes. The outer container is filled with 2 mL of 36 mM (2 g/L) potassium hydroxide aqueous solution. The outer container is hermetically closed by a stopper that causes the aseptically opening of the inner one. Containers tempering to 37 °C promotes bacteria growth and hence carbon dioxide release ($C_6H_{12}O_6 + 6O_2 \rightarrow 6CO_2 + 6H_2O$). The carbon dioxide flows from the inner container to the outer one, where it is adsorbed by the KOH solution ($CO_2 + 2HO^- \rightarrow CO_3^{2-} + H_2O$) and causes the change of the initial impedance value ($\sim$180 Ohm^{-1}). Data were acquired every 10 min.

Sample Characterization. Sample morphologies were investigated by scanning electron microscopy (SEM) using a Zeiss DSM-950 instrument. Macropore size distribution was measured using a Micromeritics Autopore II 9220 mercury porosimeter. Confocal fluorescence microscopy was performed with a Radiance 2100 (Bio-Rad) Laser Scanning System on a Zeiss Axiovert 200 microscope. Confocal fluorescent micrographs of PVA-S samples were taken on the external surface of the scaffold (see the Supporting Information, Figure S2) up to a depth of 30 μm. Confocal fluorescence micrographs of PVA-SB and PVA-SBB samples were taken on the internal surface of sliced samples (see the Supporting Information, Figure S2) with different depths of focus (20, 40, 60, and 80 μm). The average number of bacteria per square millimeter is obtained after counting 4−5 images, slicing the sample at different positions (for PVA-S, PVA-SB, and PVA-SBB samples) and focus depths (for PVA-SB and PVA-SBB samples). Images shown in Figures 2, 3, and 5 are representative of such a set of images.

Results and Discussion

The polymer scaffold structure was obtained by unidirectional freezing (at −196 °C) of a PVA buffered aqueous solution. The ice formation (hexagonal form) causes every solute originally dispersed in the aqueous solution to be segregated from the ice phase, giving rise to a macroporous structure characterized by "fences" of matter enclosing ice. The scaffolds obtained after subsequent freeze-drying show a macroporosity that corresponds to the empty areas where ice crystals originally resided (see SEM micrographs in Figure 1, left). Figure 1 (right SEM micrograph) shows the well-aligned microchannelled porous structure in the freezing direction. The freeze-dried macrostructure has a pore size distribution (measured by mercury intrusion porosimetry) of ca. 1 μm.

Our first concern was to corroborate whether or not preformed PVA scaffolds (PVA-S samples) can be entirely

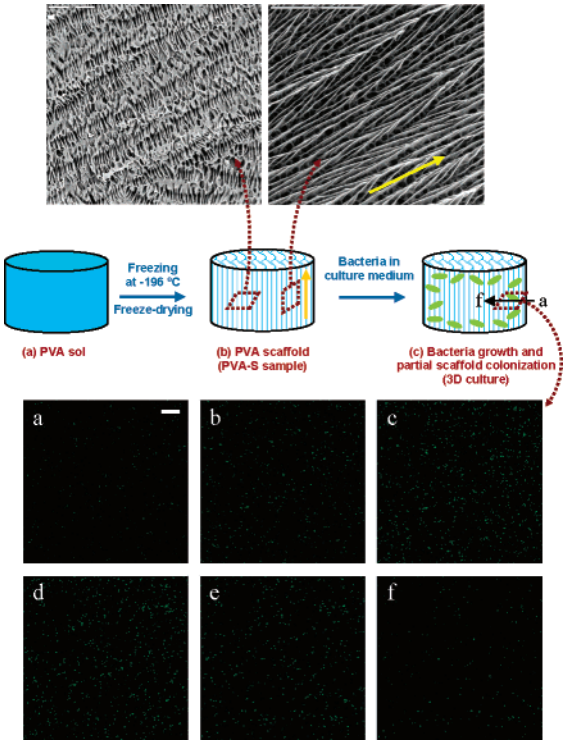

Figure 1. Scheme representing the process followed for preparation of PVA-S, SEM micrographs, and confocal fluorescence microscope images. SEM micrographs show a cross-section (left) and a longitudinal section (right, arrow indicates the direction of freezing) of the PVA scaffold (scale bars are 20 μm). Confocal fluorescence microscope images show a PVA-S sample soaked for 24 h in a suspension of bacteria in culture medium. The depth of focus was (a) the external surface and (b) 6, (c) 12, (d) 18, (e) 24, and (f) 30 μm. Bar is 20 μm.

colonized by simple soaking in a bacteria culture suspension. For this purpose, we performed confocal fluorescence images of the PVA-S sample after 24 h of soaking. Note that genetically modified bacteria emit fluorescence at 510 nm (green light) as far as they remain alive.[11] The set of confocal fluorescence images shown in Figure 1 reveals that bacteria proliferation within the scaffold was indeed limited to just a few bacteria layers in deph (up to ca. 24 μm, Figure 1a−d), with ca. 27 000 bacteria/mm^2 in the most populated layer (Figure 1d). The decrease in population observed beyond those layers (deeper than 24−30 μm, images e and f of Figure 1) is in good accord with similar experiments previously reported in different works. The most likely reason behind this feature is (as described in the introduction)[4] the poor access of the innermost bacteria to the nutrients and oxygen provided by the external medium.

To improve bacteria proliferation within the PVA scaffold, we attempted to immobilize bacteria simultaneously to the scaffold preparation. In a first approach, bacteria were immobilized by the application of the ISISA process to a PVA solution that also contains suspended bacteria (PVA-SB sample, see the scheme in Figure 2). The biocompatibility of the process was evaluated by soaking the PVA-SB sample in a medium containing glucose (see Experimental Section). Figure 3 shows that the culture medium becomes turbid after incubation at 37 °C for 24 h, which confirms the presence of viable bacteria after ISISA process. Confocal fluorescence microscopy of the PVA-SB sample reveals the colonization of the scaffold macrostructure, with ca. 22000 ± 2000

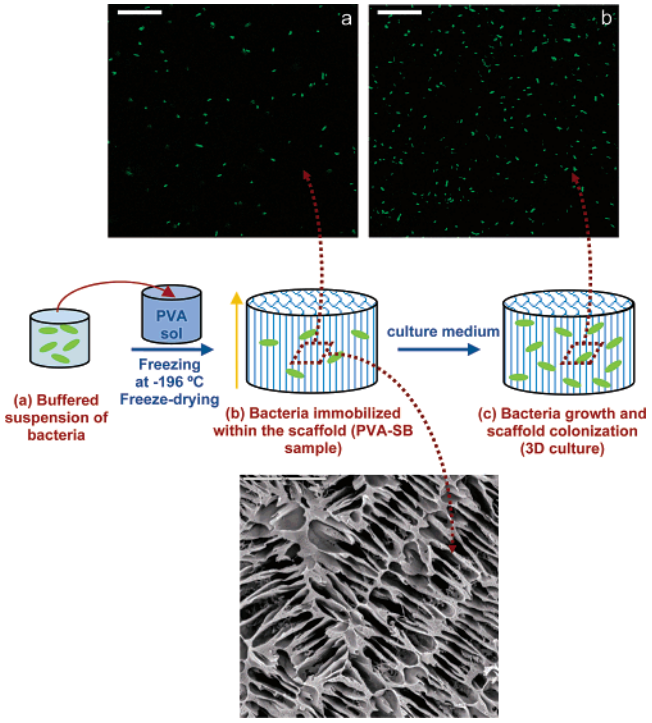

Figure 2. Scheme representing the process followed for preparation of PVA-SB, SEM micrographs, and confocal fluorescence microscope images. SEM micrograph shows a cross-section of the PVA-SB (scale bar is 10 μm). Confocal fluorescence microscope images show PVA-SB samples (a) before and (b) after soaking in culture medium and incubation at 37 °C for 24 h (scale bars are 20 μm). The homogeneous bacteria distribution within the scaffold structure is visualized in picture a. Images were taken from the internal surface of cross-sectioned PVA-SB samples (see Figure S2 in the Supporting Information) with a focus depth of 40 μm.

Figure 3. Picture of PVA-SB samples (left) right after soaking in culture medium and (right) after incubation at 37 °C for 24 h.

bacteria/mm^2 (see confocal fluorescence microscope images in Figure 2). In this case, the PVA macrostructure guaranties the easy diffusion of nutrients throughout the whole scaffold structure so that their consumption by bacteria is no longer a problem for the entire scaffold colonization, i.e., bacteria grow throughout the structure, from the inner to the outer side.

To further evaluate the proliferation of bacteria within the scaffold structure, we used a microbial indirect impedance technique that allows for monitoring cell growth within the scaffold. The method consists of the measurement of impedance changes (in percent) occurring in a potassium hydroxide solution as consequence of the absorption of the carbon dioxide resulting from the characteristic metabolic activity of bacteria (see Experimental Section for details), i.e., larger impedance changes correspond to larger bacteria

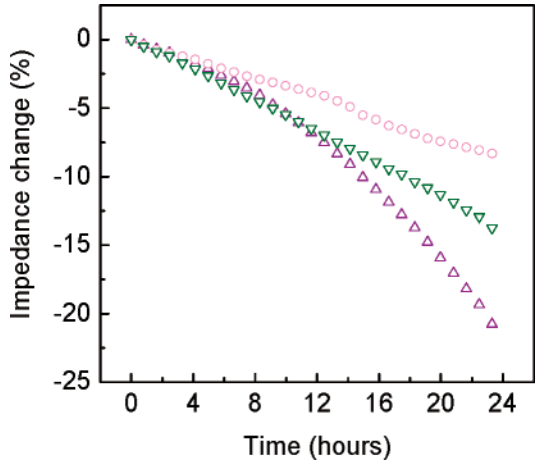

Figure 4. Plot of indirect impedance change (in %) versus incubation time in culture medium at 37 °C for PVA-SB (magenta circle) and PVA-SBB (olive inverted triangle) samples. The growth of bacteria suspended in culture medium (purple triangle) is also included for comparison. Impedance changes are related to the metabolic activity (higher CO_2 production) and hence provide a measurement of bacteria proliferation.

proliferation.[13] Impedance measurements clearly reveal a lower CO_2 production for PVA-SB samples than for bacteria suspended in culture medium (Figure 4).

This limited proliferation must be related to the cryogenic process used for immobilization. It is well-known that freezing of cellular structures is not a trivial issue and tends to damage cell membrane.[14] Damage occurs as a consequence of ice formation, which nature (e.g., extracellular or intracellular) is indeed determined by the cooling rate. Thus, extracellular ice formation occurring for slow cooling rates (below ca. 8 °C/min) results in an increase in the osmotic strength at the cells surrounding the environment. This causes dehydration and subsequent shrinkage of cells, which ultimately results in membrane disruption given that the bilayer normal structure can only be maintained down to the maximum packaging density of the lipids. Meanwhile, if the rate of cooling is faster than the rate at which the cells dehydrate, the intracellular content freezes to maintain the water equilibrium, the volume increases (note that hexagonal ice density is 0.917 g/L) and disrupts the membrane structure.[15] The formation of amorphous water (e.g., glassy water, with a density similar to that of water) would limit such effect,[16] but the required cooling rates (ca. 1×10^6 °C/s) are unaffordable with our experimental set up. The cooling rate used in our case is ca. 17 °C/min, which implies that cell damage most likely occurs by the formation of intracellular ice. Thus, reduction of cell damage during PVA scaffold formation requires cryoprotection.[17] Cryoprotectants create a high viscosity microenvironment surrounding the cells, which cause water to vitrify rather than crystallize (even at freezing rates much slower than 1×10^6 °C/s) and helps

(13) Timms, S.; Colquhoun, K. O.; Fricker, C. R. *J. Microbiol. Meth.* **1996**, *26*, 125.
(14) Withers, L. A. *The Effects of Low Temperatures on Biological Systems;* Grout, B. W. W., Morris. J. G., Eds.; Edward Arnold: London, 1987; p 389.
(15) Caffrey, M. *Biochim. Biophys. Acta* **1987**, *896*, 123.
(16) Velikov, V.; Borick, S.; Angell, C. A. *Science* **2001**, *294*, 2335.
(17) Rudge, R. H. *Maintenance of Microorganism and Cultured Cells. A Manual of Laboratory Methods*; Kirsop, B. E., Doyle, A., Eds. Academic Press: London, 1991; p 31.

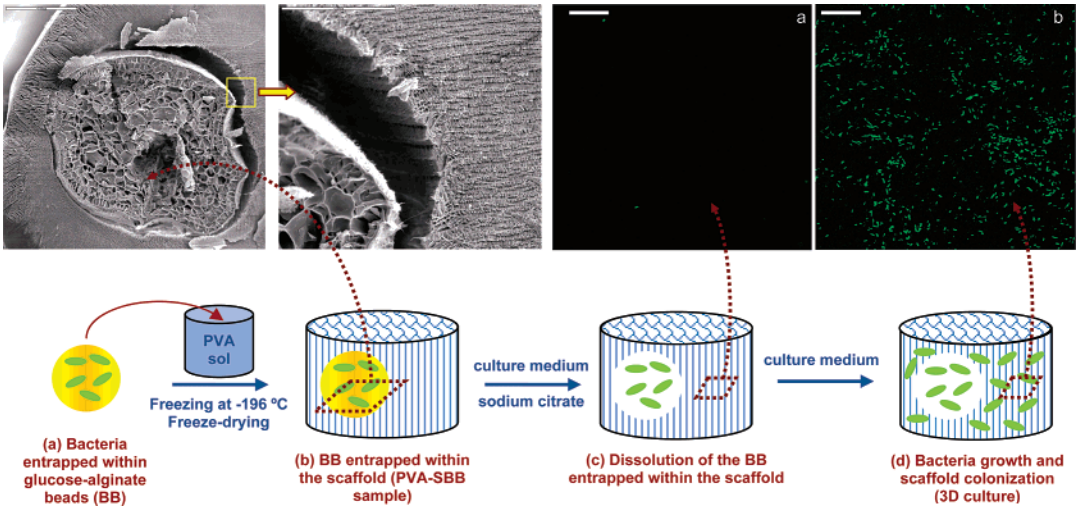

Figure 5. Scheme representing the process followed for preparation of PVA-SBB, SEM micrographs, and confocal fluorescence microscope images. SEM micrographs show a PVA-SBB sample (BB is ~1 mm diameter) prior to soaking in culture medium and bead disolution. Scale bars are (left) 500 and (right) 200 μm. Confocal fluorescence microscope images show PVA-SBB samples soaked in culture medium (a) before and (b) after incubation at 37 °C for 24 h (scale bars are 20 μm). Images were taken from the internal surface of cross-sectioned PVA-SBB samples (see Figure S2 in the Supporting Information) with a focus depth of 40 μm.

to preserve the membrane integrity upon freezing. In our case, such a role is played by the polymer matter that forms the scaffold macrostructure. However, this trend is just valid in those cases where the fence thickness of the scaffold macrostructure is able to fully embed the membrane structures.[10a,18] If one desires to standardize this cryogenic method for immobilization of cells whose size is larger than that of fences, further bacteria cryoprotection is required. For this purpose, we decided to entrap bacteria within beads composed of a natural calcium-alginate polymer also containing glucose (BB).[12] The optimum glucose concentration is found to be 20 wt= % (see the Supporting Information, Figure S3).

As described in the Experimental Section, PVA scaffolds with immobilized BB (PVA-SBB samples) are prepared by unidirectional freezing (at −196 °C) of an aqueous PVA suspension of BB (Scheme in Figure 5). The PVA-SBB samples resulting after freeze-drying (see the scheme in parts a and b of Figure 5) show BB homogeneously distributed within the characteristic micrometer-sized structure of the PVA scaffold (Figure 5). Note that at this stage (right after freeze-drying and prior soaking), bacteria are just immobilized at the BB and not yet proliferating within the PVA structure (Figure 5).

As for PVA-SB samples, the biocompatibility of the immobilization process was evaluated by soaking the PVA-SBB in a culture medium, which, in this case, also contains sodium citrate (see the scheme in parts c and d of Figure 5). Calcium chelation with citrate results in dissolution of alginate beads, turning the cavity content to liquid, which allows for bacterial dispersion and eventual growth within the PVA scaffold. Bacteria proliferation throughout the scaffold structure was studied by confocal fluorescence microscopy (Figure 5). For this purpose, the focus was at the scaffold structure and not at the BB in both images (a and b) shown in Figure 5. Thus, prior to soaking, no bacteria are observed within the scaffold structure. Meanwhile, after soaking, bacteria have successfully colonized the entire scaffold macrostructure. A close inspection to the confocal fluorescence micrograph shown in Figure 5b reveals that the bacteria population is larger for PVA-SBB than for PVA-SB (59 000 vs 22 000 ± 2000 bacteria/mm^2). Such a population is also much larger than that found for PVA-S samples (ca. 27 000 ± 2000 bacteria/mm^2), in spite of the partial colonization (in just some few layers close to the external surface) occurring in that case. This tendency is indeed corroborated by impedance measurements of PVA-SBB samples, which exhibit larger CO_2 production than that found for PVA-SB, and is closer to that for fresh bacteria suspended in culture medium (Figure 4). The above-mentioned results indicate that proliferation efficiency largely improves when BBs are used for bacterial immobilization.

Conclusions

In summary, this work demonstrates the validity of the ISISA process for the immobilization of bacteria within the macrostructure of PVA scaffolds, simultaneously with their preparation. The use of bacteria-glucose-alginate beads is capital for the preservation of the structural integrity of immobilized bacteria. Otherwise (e.g., PVA-SB samples in which bacteria are immobilized within the PVA scaffold without further cryoprotection), the viable bacteria decrease significantly, regardless of the partial cryoprotection that the polymer scaffold can eventually achieve. The results described above show the suitability of these scaffolds for 3D cultures, simply by dissolving the beads and soaking the scaffold into culture medium. Under these circumstances, both confocal fluorescence microscopy images and impedance measurements show remarkable bacteria accessibility to the whole scaffold microstructure. The current study has been achieved using PVA scaffolds and *E. coli* as culturable cells, but it is worth noting that the approach is quite versatile and besides the nature of the scaffold composition (biodegradable, biocompatible, or electron conducting, among

(18) Soltmann, U.; Böttcher, H.; Koch, D.; Grathwohl, G. *Mater. Lett.* **2003**, *57*, 2861.

others),[9] it allows for tailoring of the micrometer-sized porosity (from 20 to 100 μm) and bulk processing (different sizes and shapes, both regular and irregular; see Figures S1 and S4 in the Supporting Information). In particular, we consider that the materials prepared in this work are quite useful for those processes in biotechnology for which the efficiency of the device is ultimately determined by the bacteria growth throughout the 3D support (e.g., catalysis[1] or microbial fuel cells,[19] among others). However, we also want to emphasize that the use of alginate beads allows for entrapment of many different cells (e.g., *B. subtilis* and *S. cerevisiae*),[20] even human types.[21] These features could make this approach potentially useful for tissue engineering.

Acknowledgment. The authors thank S-0505/PPQ-0316, BMC2003-00063, 200660F0111, MAT2006-02394, and MAT2006-05979 Projects for financial support. We also acknowledge TPA Inc. and *Fundación Domingo Martínez* for valuable support. M.L.F. and M.C.G. acknowledge MEC and CSIC for postdoctoral research contracts. Fernando Pinto and Sylvia Gutiérrez are acknowledged for helpful assistance with SEM and confocal fluorescence microscopy experiments, respectively.

Supporting Information Available: Images of PVA scaffolds, fluorescence response of freeze-dried BB, SEM micrographs. This material is available free of charge via the Internet at http://pubs.acs.org.

CM062882S

(19) (a) Schröder, U.; Niessen, J.; Scholz, F. A. *Angew. Chem., Int. Ed.* **2003**, *42*, 2880. (b) Chaudhuri, S. K.; Lovley, D. R. *Nat. Biotechnol.* **2003**, *21*, 1229.

(20) Perullini, M.; Jobbágy, M.; Soler-Illia, G. J. A. A.; Bilmes, S. A. *Chem. Mater.* **2005**, *17*, 3806.

(21) Green, D. W.; Leveque, I.; Walsh, D.; Howard, D.; Yang, X.; Partridge, K.; Mann, S.; Oreffo, R. O. C. *Adv. Funct. Mater.* **2005**, *15*, 917.